ELSEVIER

Journal of Hydrology 219 (1999) 7–19

Journal of Hydrology

# The water balance of the Susquehanna River Basin and its response to climate change

R.G. Najjar*

*Department of Meteorology, The Pennsylvania State University, University Park, PA 16802-5013, USA*

Received 21 April 1998; accepted 9 March 1999

**Abstract**

Historical precipitation, temperature and streamflow data for the Susquehanna River Basin (SRB) are analyzed with the objective of developing simple statistical and water balance models of streamflow at the watershed's outlet. Annual streamflow is highly correlated with annual precipitation ($r^2 = 0.895$) and, on a percent basis, changes in annual streamflow ($\bar{Q}$) are about two times greater than changes in annual precipitation ($\bar{P}$). Variations in $\bar{P} - \bar{Q}$, interpreted as annual evapotranspiration, are much smaller than variations in $\bar{P}$ and $\bar{Q}$, and are weakly positively correlated with annual mean temperature in accordance with potential evapotranspiration formulae. Streamflow is monotonically related to diagnosed storage of water in the SRB from April through November. Deviations from this trend during winter are interpreted as changes in snowpack, and are in general agreement with climatological snow water equivalent estimates for the basin. A simple, spatially-lumped water balance model of the SRB is developed and shown to capture 99% of the mean annual cycle and 75% of the monthly streamflow from 1900 to 1987. Two ''downscaled'' predictions of precipitation and one of temperature for a doubling of atmospheric $CO_2$ are used as inputs to the statistical and water balance models of the SRB. The result is an annual streamflow increase of 24 ± 13% (11.8 ± 6.7 cm). 

*Keywords:* Water balance; Susquehanna River Basin; Numerical models; Global change; General circulation models

## 1. Introduction

Physical, chemical and biological processes in Chesapeake Bay, the largest estuary in the US, are profoundly influenced by the flow of the Susquehanna River (Schubel and Pritchard, 1986). As precipitation and temperature are strong drivers of streamflow, and as anthropogenic increases in atmospheric $CO_2$ are speculated to cause changes in precipitation and temperature, there is the potential for substantial climate-induced changes in Chesapeake Bay and other estuaries in the future. Such changes can be predicted, in principal, by coupling models of the climate, land surface hydrology and estuaries (Justić et al., 1996). Typical climate models, however, do not have the spatial resolution needed for adequate simulation of precipitation on the regional scales of interest for assessing environmental, economic and social impacts. There are currently two ways of dealing with this difficulty. One approach is to increase the resolution. Though not practical on a global scale, improved precipitation predictions can be made regionally by nesting a model of fine resolution within a coarse resolution model. A second approach is to

* Also in Department of Geosciences and Earth System Science Center. Fax: + 1-814-865-3663.

*E-mail address:* najjar@essc.psu.edu (R.G. Najjar)

0022-1694/99/$ - see front matter 
PII: S0022-1694(99)00041-4

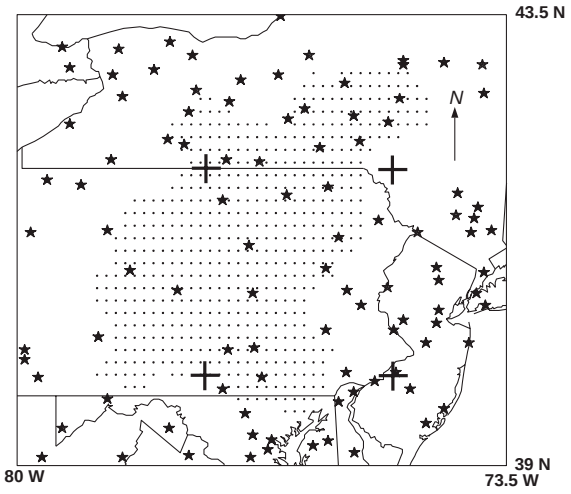


Fig. 1. Map of study area showing precipitation stations (stars) and the SRB (dots). The distribution of temperature-containing stations is similar to that of precipitation, though not identical. The centers of the grid boxes at which precipitation and temperature predictions were made for $1 \times CO_2$ and $2 \times CO_2$ are indicated by the large crosses.

develop empirical relationships between precipitation and the large-scale features of the climate that models simulate well.

Both approaches, referred to as ''downscaling'', have been adopted for regions encompassing the Susquehanna River Basin (SRB) using versions of the GENESIS atmospheric general circulation model for $1 \times CO_2$ and $2 \times CO_2$ conditions with respect to the present day concentrations (Crane and Hewitson, 1998; Jenkins and Barron, 1997; G. Jenkins, personal communication). Crane and Hewitson (1998), using empirical downscaling, predict that a $CO_2$ doubling will result in a 21% increase in annual precipitation, with the largest increases during the spring and summer. The Jenkins and Barron (1997) nested model was coupled to a simple mixed layer model of the ocean and run to steady state under $1 \times CO_2$ and $2 \times CO_2$ conditions (Jenkins, personal communication). A 13% increase in the annual precipitation is predicted, mainly during the winter and spring, in response to a doubling of $CO_2$. Significantly, both approaches predict increases in precipitation, both annually and during the spring when the streamflow has the most substantial impact on Chesapeake Bay anoxia (Seliger and Boggs, 1988). The nested model also predicts large increases in surface air temperature for all the months, with an increase of 2.5°C on average. No empirical downscaled estimates of temperature change are currently available for the SRB.

How these precipitation and temperature changes translate into predictions for Susquehanna River flow into the Chesapeake Bay is the primary objective of this article. Standard water balance techniques (Thornthwaite, 1948; Gleick, 1986) are used to predict the changes in the annual cycle in flow, as has been performed by numerous investigators for climate change applications. Linear regression is also used for predictions of annual flow changes because it is very robust. In addition, years in the historical record analogous to the $2 \times CO_2$ precipitation predictions are analyzed.

Spatial variations of parameters and processes within the SRB and temporal variations less than one month are not taken into account explicitly. Human-controlled water use and storage are also ignored in this study because they are relatively small when compared to natural processes. Jackson and Jesien (1996) have summarized water use in the SRB and report that the maximum possible storage in reservoirs is currently only 5% of the annual flow at the mouth of the Susquehanna River, and the controlled drainage area is currently only 11% of the entire basin. Consumptive water use and the diversion of water from the basin amount to only 2% of the mean flow at the mouth of the Susquehanna River.

## 2. Data sets

Daily streamflow data were retrieved from the United States Geological Survey (USGS) home page. Measurements closest to the Susquehanna River's mouth from this data source are at Conowingo Dam (USGS station number 01578310), about 15 km upstream of the mouth. This record, however, only goes back to 1967. The record at Harrisburg (USGS station number 01570500), about 100 km upstream of Conowingo Dam, extends back to 1890. Monthly means of the two records from 1967 to 1993 (the period of overlap) are highly correlated: a linear least-squares fit with a forced zero intercept has an $r^2$ of 0.993. This fit also reveals that the flow at Conowingo is higher than that at Harrisburg by 14.5% on

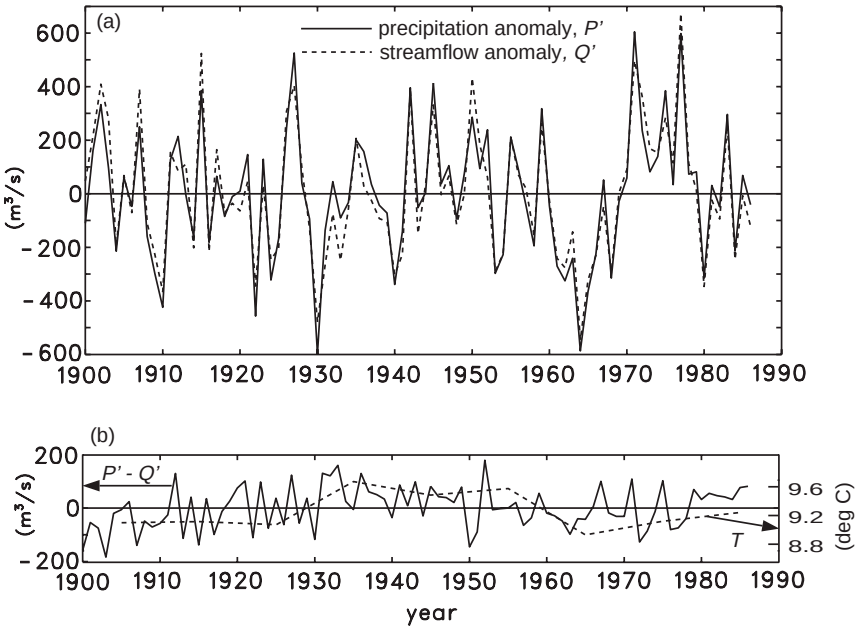


Fig. 2. (a) Anomalies of July–June water year averages of basin-mean precipitation ($P'$), and flow at the mouth of the Susquehanna River ($Q'$) from 1900–1987; (b) $P' - Q'$ and decadal averages of temperature from 1900 to 1987.

average. Throughout the remainder of this article, only streamflow data at Harrisburg multiplied by 1.145 are used and interpreted as the flow at the mouth of the Susquehanna River.

Monthly mean precipitation and temperature data were taken from the Climatological Baseline Station Data Over Land (CBSDOL) from the National Oceanic and Atmospheric Administration (Baker et al., 1994). Data sets were retrieved on-line from the internet. The time period chosen for this study, 1900–1987, is based largely on the availability of CBSDOL meteorological stations in this region. The temperature and precipitation data were binned onto a 1/8° (roughly 12 km) grid in the rectangular region bounded by 39°N, 43.5°N, 80°W and 73.5°W (Fig. 1). The grid points without observations were assigned values by numerically solving the steady state diffusion equation

$$\frac{\partial^2 A}{\partial x^2} + \frac{\partial^2 A}{\partial y^2} = 0 \tag{1}$$

where $A$ is either temperature or precipitation, $x$ is the distance to the east and $y$ is the distance to the north. Grid points with observations were used as the boundary conditions. The gridded data were then averaged over the whole SRB. The meteorological data is used only in this spatially averaged form throughout the remainder of the article.

## 3. The observed water balance of the SRB

In discussing the water budget of the SRB, four terms are considered: the change in water stored ($\mathrm{d}S/\mathrm{d}t$) in the SRB, spatially-averaged precipitation ($P$) and evapotranspiration ($E$) over the SRB, and flow at the mouth of the Susquehanna River ($Q$). These terms are related through

$$\frac{\mathrm{d}S}{\mathrm{d}t} = P - Q - E \tag{2}$$

Storage ($S$) here is defined as the total amount of water in the SRB, including, for example, soil moisture, groundwater, snow, ice, lakes and rivers. In addition to ignoring human water use, Eq. (2) also assumes that groundwater leakage across the boundaries of the SRB is minimal.

### 3.1. Long term average

Defining whole-record averages with the symbol $\langle\ \rangle$, it is found that $\langle P\rangle = 1.0\ \mathrm{m\ yr^{-1}}$, equivalent to a flow rate of $2250\ \mathrm{m^3\ s^{-1}}$, considering the area of the SRB ($71250\ \mathrm{km^2}$), and $\langle Q\rangle = 0.49\ \mathrm{m\ yr^{-1}}$ ($1100\ \mathrm{m^3\ s^{-1}}$). Making the reasonable assumption that the mean storage change from 1900 to 1987 is negligible, use of Eq. (2) reveals that 0.51 m of evapotranspiration occur annually ($1150\ \mathrm{m^3\ s^{-1}}$) from the SRB on average.

### 3.2. Year-to-year variations of annual averages

To determine the most appropriate annual averaging period for relating flow to meteorology, annual averages of precipitation and streamflow were computed for *all* 12-month periods in the record (January–December, February–January, etc.). Twelve least-squares linear regressions were performed, one for each 12-month period ($n = 87$). The highest correlation between annual $P$ and $R$ is when the averaging is from July to June ($r^2 = 0.895$). The standard water year (October–December) shows, surprisingly, a significantly lower correlation ($r^2 = 0.686$), as does the calendar year ($r^2 = 0.767$), which is often used in the Eastern United States. One possible explanation for this is that soils may normally be saturated by the end of June. By the end of September, however, soils could be saturated or completely dry, depending on the cumulative effects of summertime meteorological conditions. Thus, changes in the storage from one standard water year to the next could be considerable. Calendar year correlations are lower probably because of variations in snow storage from year to year.

Defining July–June water year averages with an overbar, the least squares linear fit of $\bar{Q}$ ($\mathrm{m^3\ s^{-1}}$) as a function of $\bar{P}$ ($\mathrm{m^3\ s^{-1}}$) is given by

$$\bar{Q} = -1007 + 0.937\bar{P} \tag{3}$$

which has a standard deviation of $78\ \mathrm{m^3\ s^{-1}}$. Adding temperature as an independent variable and incorporating lags (for both $\bar{P}$ and $\bar{T}$) increases $r^2$ by only an additional 0.03. July–June water year precipitation and streamflow anomalies, $P'$ and $Q'$, respectively, defined as the annual average minus the long term mean ($x' = \bar{x} - \langle x\rangle$), are almost equal (Fig. 2(a)). A convenient way of expressing the sensitivity of flow to precipitation is with an ''amplification'' factor, $\beta$ (Karl and Riebsame, 1989)

$$\beta = \frac{Q'/\langle Q\rangle}{P'/\langle P\rangle} \tag{4}$$

Using Eq. (3), the definition of $x'$, and noting that Eq. (3) is satisfied by the long-term averages, it is found that $\beta = 0.937\langle P\rangle/\langle Q\rangle = 1.92$. Thus, fractional changes in the annual streamflow are about two times fractional changes in the annual precipitation.

If it is assumed that storage changes are negligible from year to year, and if we accept Eq. (2), then the annual evapotranspiration anomaly is equal to $P' - Q'$, which shows little interannual variability compared to $P'$ and $Q'$ individually (Fig. 2(b)); standard deviations of $P'$ and $Q'$ are 242 and $240\ \mathrm{m^3\ s^{-1}}$, respectively, while the standard deviation of $P' - Q'$ is only $79\ \mathrm{m^3\ s^{-1}}$. Why should this be the case? It is surprising, for example, that $P' - Q'$ is not significantly different between the 1960s and the 1970s, the driest and wettest decades, respectively, in the record presented here. Other factors that affect evapotranspiration, such as humidity, solar radiation, temperature and wind speed, have interannual variability, but do not seem to be reflected in $P' - Q'$. For example, the following linear regression of $\bar{P} - \bar{Q}$ ($\mathrm{m^3\ s^{-1}}$) versus temperature (°C) explains only 11% of the variability in $\bar{P} - \bar{Q}$

$$\bar{P} - \bar{Q} = 760.4 + 41.97\bar{T} \tag{5}$$

One possible explanation for this constancy is that climatic variables could have conflicting effects on evapotranspiration (e.g. wet summers are likely to be cooler). Another possibility is that trees, which dominate the vegetation of the SRB, have deep root systems and are therefore relatively insensitive to soil moisture.

Although $\bar{P}$ and $\bar{Q}$ have no long-term trends that are clearly apparent, $\bar{P} - \bar{Q}$ does show long term trends: an increase from 1900 to the early 1930s, followed by a long term decrease until 1970, after which there is an increase to 1987, the end of the record. Decadal average air temperature for the SRB shows a similar trend (Fig. 2(b)), and 28% of the variability in decadal average $P - Q$ ($\mathrm{m^3\ s^{-1}}$) can be captured with a least-squares linear fit as a function of decadal average

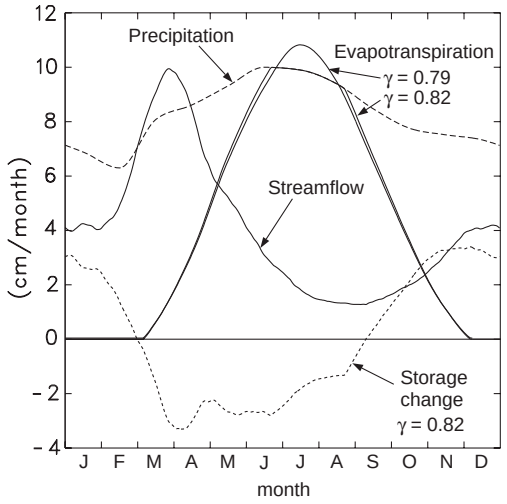


Fig. 3. Mean annual cycle of the integrated SRB water balance from 1900 to 1987. Flow at the mouth of the Susquehanna River is a 31-day running mean. Monthly precipitation and evapotranspiration have been interpolated using the scheme of Steffen (1990). The two formulations of evapotranspiration are described in the text. Storage change was computed for $\gamma = 0.82$ using Eq. (2) in the text.

temperature (°C): $P - Q = 211 + 101T$ ($n = 9$). (Adding precipitation or considering only summertime temperature does not improve the correlation.) This relationship suggests a sensitivity of evapotranspiration to temperature of 10% $°C^{-1}$, while the relationship on annual time scales (Eq. (5)) is 4% $°C^{-1}$. This range, 4–10% $°C^{-1}$, is the same as the range given by eight formulations of potential evapotranspiration (McKenney and Rosenberg, 1993), and hence it seems likely that changes in the annual temperature are causing changes in the annual evapotranspiration. This is not to say that other factors may not be important in the long term trends in $\bar{P} - \bar{Q}$, such as changes in land use and the direct effects of $CO_2$ on the biosphere.

### *3.3. The mean annual cycle*

Although highly correlated on interannual time scales, precipitation and streamflow are decoupled on seasonal time scales (Fig. 3). The flow at the mouth of the Susquehanna River has a strong mean annual cycle with a peak near the end of March and a minimum near the end of August. Precipitation, on the contrary, has a weak mean annual cycle with higher values in the early summer and a minimum in winter. Storage and evapotranspiration are responsible for the decoupling of precipitation and streamflow. The strong seasonal cycle of potential evapotranspiration, with a maximum during summer, causes streamflow to be a minimum at this time in spite of the mild maximum in precipitation. Storage of water in the basin as snow during winter and melting during the spring help to contribute to the streamflow peak, when precipitation is near its average value.

## 4. Relationship between storage and streamflow

To constrain the relationship between streamflow and storage for the SRB, a simple diagnostic water balance model is developed. The main problem is to determine evapotranspiration. In standard water balance methods, evapotranspiration is assumed to proceed at its potential ($E_p$) as long as the soil is wet. If the soil is completely dry, then evapotranspiration is assumed to equal precipitation, the only source of available water. The soil is assumed to have a maximum water holding capacity $S_s^0$, which when exceeded, causes water to be diverted to a runoff reservoir. From the diagnostic point of view, there is an additional constraint on evapotranspiration in a basin: assuming storage changes are negligible over the long term, the average evapotranspiration must be equal to the average of basin-mean precipitation minus streamflow at the basin's outlet. Formulations of $E_p$ differ greatly, but have a similar seasonal shape (Jensen et al., 1990), hence the approach here is to employ a multiplicative factor $\gamma$ to adjust the potential evapotranspiration formulation of Thornthwaite (1948) in order for the annual water budget to be balanced. If evapotranspiration proceeds at its potential throughout the year, then, in order to balance the annual water budget, $\gamma$ must be equal to 0.79. In this case (Fig. 3), the summer soil moisture deficit (excess of evapotranspiration over precipitation) is only about 1 cm, relatively small when compared to reasonable estimates of the mean soil moisture capacity averaged over the SRB. Thus, the soil will not dry out, on average, and evapotranspiration will proceed at its potential, as assumed.

It seems likely, however, that evapotranspiration will occasionally be limited by soil moisture in the

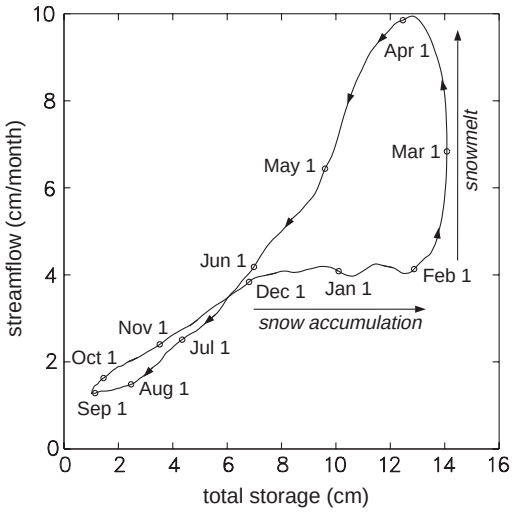


Fig. 4. Relationship between storage and streamflow for the SRB mean annual cycle.

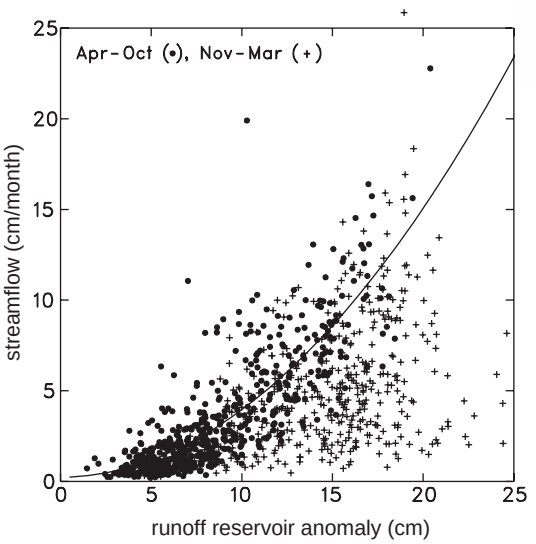


Fig. 5. Relationship between storage and streamflow for the full SRB record (1900–1987). Each point represents one month. See text for details. The curve is a least squares parabolic fit through the April–October points.

SRB. For example, the four driest years in the record (1910, 1922, 1930 and 1964) have below-normal $\bar{P} - \bar{Q}$ (Fig. 2). Thus, it is reasonable to assume that summertime average evapotranspiration for the whole record (1900–1987) will be somewhat lower than the potential, even though for most years the potential might be achieved. To simulate this for an extreme case, the maximum soil moisture capacity is assumed to be zero. Thus, evapotranspiration is set equal to precipitation during the summer months, when $E_p$ exceeds $P$. In order to balance the annual water budget in this case, $\gamma$ must be equal to 0.82.

For the computed storage change, only the case with $\gamma = 0.82$ is shown in Fig. 3, but in both cases water accumulates in the SRB during fall and winter and is lost from the SRB during spring and summer. In Fig. 4, streamflow is plotted versus total storage, computed by integrating the storage change in Fig. 3. An arbitrary value of 10 cm was chosen for storage on January 1. It is seen that streamflow increases essentially monotonically with inferred storage from the beginning of April to the end of November, two-thirds of the year. Since this period is essentially devoid of snow, the changes in storage during this time must reflect changes in liquid storage reservoirs, such as groundwater.

Substantial deviations from the monotonic streamflow–storage trend occur during the winter. During December and January, inferred storage increases with little change in the streamflow. This most likely represents an increase of water in the SRB as snowpack. During February and March, storage changes are small, but streamflow more than doubles, returning to the monotonic streamflow–storage curve. This increase in streamflow most likely reflects the melting of snow. The maximum snow water-equivalent (SWE) can be estimated from Fig. 4 to be the maximum departure of winter storage from the April–November streamflow–storage relationship, about 6 cm. How does this compare with observations? A visual inspection of the median seasonal maximum SWE map for the Northeastern US (Wilks and McKay, 1994) reveals that the average over the SRB is about 4 cm, somewhat less than that diagnosed from the water balance. The difference may be because $E_p$ predicted by the Thornthwaite formula is too low in winter (McCabe, 1989) or that the SWE estimate is too low due to a topographic bias associated with the fact that most snow measurement stations in mountainous regions are located in valleys (Wilks and McKay, 1994).

How does the storage–flow relationship look for regimes outside the average annual cycle shown in

Fig. 4? To investigate this, monthly evapotranspiration was computed for the full record (1900–1987) in the same manner as for the mean annual cycle. To balance the long term water budget, $\gamma$ must be equal to 0.79 and 0.93 for $S_s^0$ equals to 10 cm and 0, respectively. Similar to the mean annual cycle calculation, storage change, d$S$/d$t$, is computed using Eq. (2) with the full record of $P$, $Q$ and computed $E$. Storage is then computed by integrating d$S$/d$t$, initializing storage (arbitrarily) at 10 cm at the beginning of the record (January 1, 1900). In addition to a prominent annual cycle, the computed storage (with $\gamma = 0.93$ and $S_s^0 = 0$) has large long term trends (not shown) that are most likely not real. To remove these trends, a 13-month moving average is subtracted from $S$. When streamflow is plotted versus the resulting storage anomaly, a picture similar to that seen for the annual cycle emerges (Fig. 5). As with the mean annual cycle, there is a non-linear relationship between storage and streamflow from the spring through the fall. The mean slope over the streamflow range of the mean annual cycle (1–10 cm mon$^{-1}$) is very close to that of the mean annual cycle itself. A least-squares parabolic fit through the April–October values yields an $r^2$ of 0.70 and a standard deviation of 1.7 cm mon$^{-1}$. Surprisingly, fits show less significance when non-zero values of $S_s^0$ are used to compute diagnosed storage in the runoff reservoir, though the differences are slight. Winter storage is generally higher than the spring-fall trend, presumably reflecting snow, similar to the mean annual cycle.

## 5. A simple water balance model of the SRB

The structure of the prognostic water balance model used here is identical to the diagnostic model used in the previous section, with the addition of a simple snow model. Precipitation is partitioned into snow and rain depending on the monthly mean air temperature. Given that large variations in temperature can occur throughout the month and throughout a typical mid-latitude basin (Gleick, 1987), the fraction of precipitation that is snow is allowed to vary continuously as a function of temperature ($T$). For $T$ less than $-\Delta T$, the snow fraction is assumed to be 1, and for $T$ greater than $+\Delta T$, the snow fraction is assumed to be zero, where all the temperatures are in °C. Between these two temperatures, the snow fraction is assumed to vary linearly with temperature. Snowfall enters the snow pack reservoir ($S_p$) and rain enters the soil reservoir ($S_s$). Melting of snow removes water from the snow reservoir and places it in the runoff reservoir ($S_r$). The rate of melting is linear in the amount of snow:

$$\text{snowmelt} = \frac{S_p}{\tau} \tag{6}$$

where $\tau$ is the snow lifetime. $\tau$ is modeled as a decreasing function of temperature only

$$\tau = \tau^0 \exp\left(-\frac{T}{T^*}\right) \tag{7}$$

where $\tau^\circ$ is the snow lifetime at 0°C and $T$ and $T^*$ are in units of °C. $T^*$ characterizes how rapidly the snow lifetime decreases with increasing temperature. This formulation is qualitatively similar to that used by Gleick (1987).

The relationship between streamflow and storage in the runoff reservoir is taken from the diagnostic model. A piecewise linear function is used that corresponds closely to the streamflow–storage relationship from September through April shown in Fig. 4, adjusting $S_r$ to ensure a zero intercept

$$Q = \frac{S_r}{2.4 \text{ mon}} \qquad S_r < 9.3 \text{ cm} \tag{8}$$

$$Q = \frac{9.3 \text{ cm}}{2.4 \text{ mon}} + \frac{S_r - 9.3 \text{ cm}}{0.9 \text{ mon}} \qquad S_r > 9.3 \text{ cm}$$

All simulations were conducted with a one-day timestep in order to capture the streamflow peak at the end of March (Fig. 3). Temperature and precipitation inputs to the model were linearly interpolated to the model timestep. Simulations of the mean annual cycle were run until a repeating cycle was found, typically within a few years. Simulations of the 1900–1987 time period were initialized with output from the mean annual cycle model.

### 5.1. Simulation of the mean annual cycle

Regardless of the values of the snow parameters, it was found that simulations of the mean annual cycle were insensitive to $S_s^0$ greater than about 1 cm, which is the summer moisture deficit. Searching the snow parameter space for values of $S_s^0$ of 0 and 1 cm

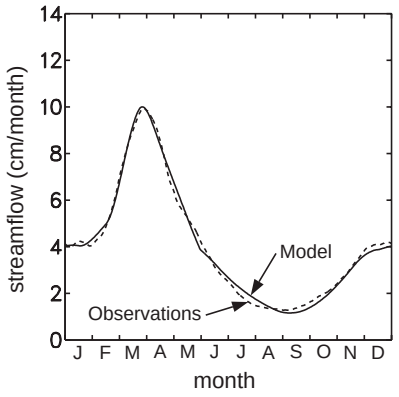


Fig. 6. Observed and modeled mean annual cycle of flow at the mouth of the Susquehanna River. Observations are as in Fig. 3.

(with $\gamma$ adjusted accordingly) revealed that the best fit to observations was with $T^* = 4.8°C$, $\tau° = 0.54$ months, $\Delta T = 3.5°C$, $S_s^0 = 0$, and $\gamma = 0.82$. The simulation with these parameters captures the mean annual cycle of flow at the mouth of the Susquehanna River very well (Fig. 6), with $r^2 = 0.993$ ($n = 365$). The fact that simulations with $S_s^0 = 0$ were slightly more skillful (mainly during the summer) than those with $S_s^0 = 1$ cm, suggests that some drying out of the soil occurs on average in the summer, as suggested earlier.

### 5.2. Simulation of interannual variability

Using the same parameter values from the mean annual cycle simulation above, $\gamma$ must equal 0.90 to balance the water budget for simulating the full record (1900–1987). The square of the correlation coefficient for this simulation, based on comparison with monthly mean values of streamflow is 0.747 ($n = 1056$). In general, the streamflow predicted by the SRB water balance model is slightly flatter than the observations, with the predicted streamflow too high during the summer low-flow period and too low during the spring high-flow period (not shown). The mean annual cycle of streamflow is responsible for 51% of the variability of monthly mean streamflow from 1900 to 1987. Thus, the model is effectively capturing about half of the variability in the monthly mean streamflow anomaly (the difference from the mean annual cycle). This is reflected in $r^2$ values for each month, which average about 0.5 (Fig. 7). Skill is lowest in the summer, when soil moisture is variable, and late winter, when snowpack is variable.

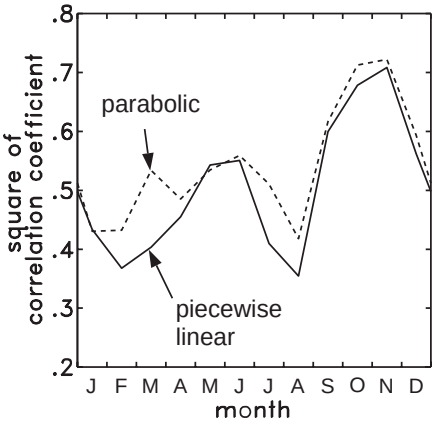


Fig. 7. Square of the correlation coefficient by month for two simulations with the interannual model. The piecewise linear model uses Eq. (8) and the parabolic model uses Eq. (9).

The skill of the interannual simulation can be improved by using the streamflow–storage relationship determined from the diagnostic calculations of the interannual water budget in Section 4. Ignoring the small intercept (0.23 cm mon$^{-1}$) in the least-squares fit in Fig. 5 yields the following relationship

$$Q = 0.00385S_r + 0.0369S_r^2 \quad (9)$$

where $Q$ is in units of cm mon$^{-1}$ and $S_r$ is in units of cm. Optimizing the snow parameters for the interannual model with this streamflow–storage relationship, $S_s^0 = 0$ and $\gamma = 0.93$ yields: $\Delta T = 1.5°C$, $\tau° = 0.38$ months, $T^* = 2.4°C$. Although $r^2$ for this simulation (0.773) is only slightly higher than that of the simulation using the parameters from the mean annual cycle model, the model no longer has the flat response discussed earlier (not shown). Accordingly, $r^2$ values for individual summer and winter months are significantly higher (Fig. 7).

## 6. Streamflow prediction for a doubling of atmospheric $CO_2$

The change in the annual streamflow resulting from the increase in the annual precipitation predicted for the SRB by the climate models can be estimated using the amplification factor for the SRB (Eq. (4)). It is found that a 17.5% (17.5 cm) increase in annual

Table 1
Years in the top 25th percentile for annual (July–June water year) precipitation. $P'$, $Q'$ and $T'$ are the annual anomalies of precipitation ($m^3\ s^{-1}$), streamflow ($m^3\ s^{-1}$) and temperature (°C), respectively. $f$ is the fraction of the annual precipitation anomaly that occurs in the corresponding six-month period. Note that 1971 and 1974 appear in both the April–September and January–June categories

| Year | $P'$ | $Q'$ | $T'$ | $f$ | $\beta$ |
|---|---|---|---|---|---|
| *50% or more of $P'$ in April–September* | | | | | |
| 1912 | 213 | 85 | 0.96 | 0.66 | 0.81 |
| 1915 | 384 | 523 | − 0.52 | 1.01 | 2.78 |
| 1921 | 145 | 45 | 0.50 | 0.70 | 0.63 |
| 1926 | 244 | 307 | − 0.40 | 0.54 | 2.57 |
| 1942 | 395 | 387 | − 0.07 | 0.69 | 2.00 |
| 1945 | 412 | 332 | 0.29 | 0.99 | 1.65 |
| 1971 | 603 | 495 | 0.02 | 0.91 | 1.68 |
| 1974 | 138 | 151 | 0.03 | 0.88 | 2.24 |
| 1975 | 384 | 283 | 0.74 | 0.88 | 1.51 |
| Average | 324 | 290 | | | 1.83[a] |
| *50% or more of $P'$ in January–June* | | | | | |
| 1935 | 200 | 206 | − 0.37 | 0.62 | 2.11 |
| 1936 | 156 | 28 | 0.54 | 1.26 | 0.37 |
| 1952 | 238 | 60 | 1.06 | 0.74 | 0.51 |
| 1971 | 603 | 495 | 0.02 | 0.84 | 1.68 |
| 1972 | 234 | 362 | 0.16 | 0.59 | 3.16 |
| 1974 | 138 | 151 | 0.03 | 1.02 | 2.24 |
| 1983 | 295 | 255 | − 0.37 | 0.82 | 1.77 |
| Average | 266 | 222 | | | 1.71[a] |
| *Other* | | | | | |
| 1901 | 160 | 215 | − 0.02 | | 2.74 |
| 1902 | 332 | 408 | 0.69 | | 2.51 |
| 1907 | 249 | 390 | − 0.23 | | 3.20 |
| 1927 | 524 | 403 | − 0.20 | | 1.57 |
| 1950 | 285 | 431 | 0.14 | | 3.09 |
| 1955 | 210 | 210 | − 0.10 | | 2.05 |
| 1959 | 317 | 262 | 0.55 | | 1.69 |
| 1977 | 597 | 672 | − 0.87 | | 2.30 |
| Average | 334 | 374 | | | 2.29[a] |

[a] Computed from the average values of $P'$ and $Q'$.

precipitation, the average of the two climate models, will result in a 33.6% (16.5 cm) increase in the annual flow at the mouth of the Susquehanna River. To estimate the streamflow response to increasing temperature, the relationship between $\bar{P} - \bar{Q}$ and $\bar{T}$ in Eq. (5) is used. With an increase of 2.5°C and no precipitation change, $\bar{P} - \bar{Q}$ will increase and therefore $\bar{Q}$ will decrease by 4.7 cm $yr^{-1}$. Thus, the total predicted increase in annual streamflow is 16.5 − 4.7 = 11.8 cm (24%).

A rough estimate of the error in this prediction can be made by considering how the errors in the following affect the predicted streamflow: (1) the precipitation prediction of the GCMs, (2) the temperature prediction of the nested climate model, (3) the linear relationship between $\bar{Q}$ and $\bar{P}$, and (4) the linear relationship between $\bar{Q}$ and $\bar{T}$. Lacking other means to determine the GCM precipitation error, it is assumed to be one-half the difference between the two GCM results, or 4.0 cm $yr^{-1}$, which translates into an error in $\bar{Q}$ of $0.937 \times 4.0$ cm $yr^{-1}$, where 0.937 is the slope of the $\bar{Q}$ versus $\bar{P}$ linear fit (Eq. (3)). The error in the GCM prediction of temperature is, rather arbitrarily, taken to be 1.0°C. Most GCMs predict warming in the Northeast US in response to increased fossil fuel burning, even when sulfate aerosols (which cool significantly, especially in Northeast US) are included in the model (e.g. Mitchell et al. 1995; Meehl and Washington, 1996). This error is propagated to streamflow using the slope of the linear fit of $\bar{P} - \bar{Q}$ versus $\bar{T}$. (Eq. (5)), to determine an error of 1.9 cm $yr^{-1}$. The errors in the linear fits are taken to be the standard deviations of Eqs. (3) and (5), which are both 3.5 cm $yr^{-1}$. Treating these four errors as random yields a total error in the annual streamflow change of 6.5 cm. Thus the predicted change in the annual streamflow is 11.8 ± 6.7 cm, or 24 ± 13%.

In making predictions of the annual mean streamflow, does it matter when the additional precipitation occurs? It might be expected, for example, that a precipitation increase in the summer, when soils tend to be relatively dry, would be less effective at producing runoff than a precipitation increase during winter. To examine this, years in the historical record analogous to the precipitation predictions of the climate models were examined. The July–June water years in the top 25th percentile of annual precipitation were selected, a total of 22 individual years (Table 1). Of these, it was determined whether 50% or more of the annual precipitation anomaly ($P'$) occurred between January and June (analogous to the nested model) or April and September (analogous to the empirical downscaled model). The average amplification factor for the 22 wettest years as well as for each analog category (January–June, April–September, and others) was computed from the corresponding mean values of $Q'$ and $P'$. The average $\beta$ for the 22 wettest years is 1.99, slightly higher than the mean $\beta$ for all the years (1.92). Mean values of $\beta$ for years with additional precipitation in January–June

Table 2
Summary of monthly and annual climate and streamflow predictions for the Susquehanna River Basin in response to a doubling of atmospheric $CO_2$. Climate models are indicated by: C&H = Crane and Hewitson (1998) empirical downscaling, Jenkins = G. Jenkins (personal communication) nested limited area model. The error shown in the lower panel is the error due to the water balance model, which was derived from simulations of interannual variability (see text)

| | J | F | M | A | M | J | J | A | S | O | N | D | Annual |
|---|---|---|---|---|---|---|---|---|---|---|---|---|---|
| *Change in precipitation (P) and temperature (T) predicted by climate models* | | | | | | | | | | | | | |
| $\Delta P$, Jenkins (%) | 38.5 | − 12.2 | 42.7 | 54.1 | 65.4 | 29.3 | − 6.1 | − 12.6 | 14.5 | − 1.7 | − 13.7 | 37.5 | 13.5 |
| $\Delta T$, Jenkins (°C) | 2.2 | 1.7 | 1.9 | 3.0 | 1.9 | 4.1 | 2.8 | 3.6 | 2.2 | 2.5 | 1.9 | 2.1 | 2.5 |
| $\Delta P$ C&H (%) | 2.1 | 10.3 | − 0.7 | 19.2 | 51.3 | 36.6 | 25.8 | 28.2 | 37.2 | 9.6 | 9.6 | 14.5 | 21.5 |
| *Percent change in streamflow predicted for the mean annual cycle model* | | | | | | | | | | | | | |
| Jenkins *P* | 29.9 | 26.3 | 23.1 | 44.0 | 91.2 | 111.1 | 58.7 | 55.4 | 51.0 | 30.8 | 6.8 | 16.7 | 43.0 |
| Jenkins *T* | 20.9 | 11.5 | − 10.1 | − 17.5 | − 14.6 | − 12.2 | − 13.8 | − 14.1 | − 24.3 | − 19.9 | − 10.7 | 3.6 | − 7.1 |
| Jenkins *P* &*T* | 60.7 | 37.9 | 10.4 | 23.5 | 73.8 | 75.9 | 36.7 | 36.3 | 23.7 | 9.6 | − 4.4 | 24.3 | 33.5 |
| C&H *P* | 22.7 | 10.8 | 6.3 | 11.3 | 49.2 | 87.7 | 78.2 | 115.3 | 163.8 | 111.5 | 78.0 | 49.1 | 41.6 |
| C&H *P*, Jenkins *T* | 45.6 | 22.8 | − 4.6 | − 7.1 | 33.0 | 52.8 | 39.4 | 45.4 | 79.6 | 60.7 | 40.0 | 53.7 | 25.6 |
| Error | 45.3 | 45.1 | 32.8 | 29.3 | 30.5 | 53.5 | 56.9 | 52.8 | 55.3 | 52.0 | 36.6 | 41.0 | – |

and April–September are 1.83 and 1.70, respectively, suggesting that these years are slightly less efficient at producing runoff than the average year. In only a few extreme cases (1912, 1921, 1936 and 1952), less than half of the expected streamflow is produced. These years, however, have relatively small values of annual precipitation (compared to the other years in the top 25th percentile), so the error in computing $P'$ and $\beta$ is relatively large. These years are also anomalously warm (Table 1), suggesting that some of the inefficiency at producing runoff is due to increased evapotranspiration. Analysis of the precipitation anomaly at three-month periods, as opposed to the six-month periods shown in Table 1, did not reveal any obvious trends. Thus, surprisingly, annual streamflow is only slightly sensitive to the timing of precipitation, at least for wet years. This supports the notion that soils in the SRB, even in the summer, are generally still wet enough to effectively produce runoff. The annual streamflow predictions made earlier, therefore, do not require any adjustment that accounts for the timing of precipitation.

A monthly-resolved prediction of the streamflow change can be made using the water balance model

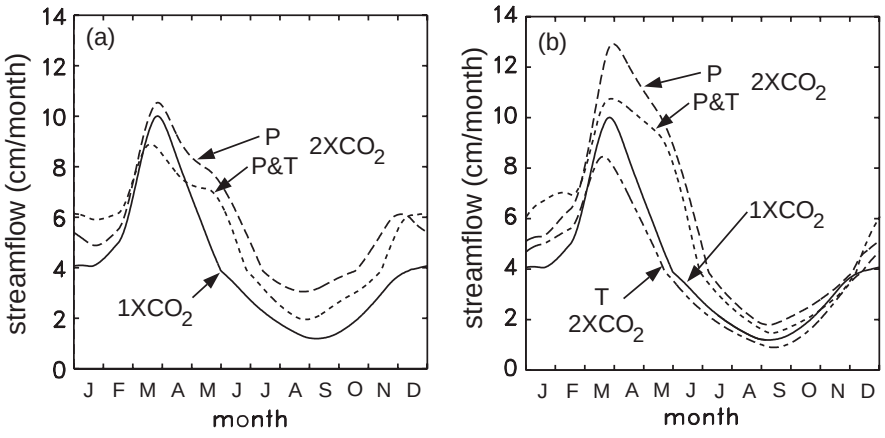


Fig. 8. Five model simulations of flow at the mouth of the Susquehanna River due to a doubling of atmospheric $CO_2$ ($2 \times CO_2$) compared to the modern day ($1 \times CO_2$). In (a), the $2 \times CO_2$ simulations use the precipitation prediction from empirical downscaling with (*P* and *T*) and without (*P*) the temperature prediction from the nested model. In (b), the $2 \times CO_2$ simulations use predictions from the nested model only.

of the mean annual cycle developed in Section 5. The water balance model was run with the observed precipitation adjusted by the *percent* changes predicted by each climate model. The water balance model was also run with the observed temperature adjusted by the *absolute* change predicted by the nested model (Table 2). Five scenarios are examined: the two precipitation predictions (one for each climate model), the temperature prediction of the nested model, and the combinations of precipitation of each model with temperature from the nested model (Table 2, Fig. 8). The error in these monthly predictions is taken to be the RMS error of the interannual model run with the same parameters as the mean annual cycle model, except with $S_s^0 = 3$ cm. Unfortunately, the predicted changes in the monthly streamflow are of the same magnitude of the error in most cases. Thus, the results of the model are more appropriately thought of as sensitivity analyses as opposed to predictions.

For each of the four scenarios that include precipitation changes, streamflow increases during almost every month. For the precipitation-only scenarios, the greatest percent increases in streamflow occur towards the end of the period of increased precipitation: late summer for the empirical downscaling and late spring for the nested model. In both cases, monthly streamflow more than doubles at this time. The annual mean increase in the streamflow for both precipitation-only cases is about the same ( $\sim$ 40%). The increase in response to the empirical downscaled precipitation is consistent with the linear regression of annual streamflow versus annual precipitation (Eq. (3)), but the increase in response to the nested model precipitation is larger than the regression would suggest. This is because evapotranspiration has actually decreased for the nested model simulation as a result of the slightly lower precipitation during July and August.

The effect of the nearly uniform temperature increase predicted by the nested model is to increase the streamflow during the winter by decreasing the amount of water in the snowpack. This then causes decreases in spring streamflow. Summer and fall decreases in streamflow occur in response to increased evapotranspiration. The annual mean streamflow decreases by about 7% in response to the temperature change, or about 3% $^{\circ}C^{-1}$, only slightly lower than expected from the statistical relationship between annual $\bar{P} - \bar{Q}$ and $\bar{T}$ discussed earlier (Eq. (5)). $E_p$ increases by 15% due to the temperature change, and one would expect the same percent decrease in the streamflow if $E = E_p$, because $\langle E \rangle$ and $\langle Q \rangle$ are nearly equal for $1 \times CO_2$ conditions. The smaller decrease in streamflow merely reflects that evapotranspiration is occurring at less than its potential.

The combined effect of changing precipitation and temperature on the annual mean flow is linear for the nested model case, but not for the case combining the empirical downscaled precipitation and the nested model temperature. For the latter, potential evapotranspiration is achieved during the summer, due to the increased summer precipitation, unlike the $1 \times CO_2$ case. The predicted increase in the annual streamflow by the two combined models is 25.6 and 33.5%, within the range predicted by the statistical model.

## 7. Conclusions

An important finding of this study, based on both the analysis of the historical data and the simple water balance modeling of the SRB, is that percent changes in the annual streamflow are about twice as large as percent changes in the annual precipitation, and the correlation between the two is very high if the averaging period is July to June. Therefore any significant changes in precipitation over the SRB resulting either from natural variability or anthropogenic climate change are likely to have a substantial impact on flow at the mouth of the Susquehanna River, and thus on the Chesapeake Bay. Temperature, on the contrary, shows only a very slight negative correlation with streamflow.

The high correlation between the annual precipitation and the annual streamflow makes it straightforward to use climate model precipitation predictions to predict changes in the annual streamflow. The assumption of a constant amplification factor is given support by its constancy (Table 1) in the face of a range of climatic variability, in terms of precipitation and temperature, during this century that is larger than the difference between $1 \times CO_2$ and $2 \times CO_2$ predictions for the SRB. Given such predictions of precipitation from two downscaled climate models, and temperature from one of these, it is estimated that annual flow at the mouth of the Susquehanna River

will increase by 24 ± 13%. This prediction is consistent with the change in the annual streamflow using a simple water balance model.

Despite large variations in the annual precipitation, the difference between the annual precipitation and the annual streamflow, interpreted to be annual evapotranspiration, has been remarkably small. This is consistent with a finding by Church et al. (1995) that $\bar{P} - \bar{Q}$ for (standard) water year 1984, which was anomalously wet, was not much different than the long-term mean of $\bar{P} - \bar{Q}$ in the Northeast US. Constancy in annual evapotranspiration for the SRB means, for example, that during anomalously wet years, the additional precipitation will mostly end up in the Chesapeake Bay. Unlike precipitation and streamflow, there are small secular trends in evapotranspiration that are only partially explained by temperature and precipitation.

Another finding of this study is that streamflow at the mouth of the Susquehanna River is monotonically and nonlinearly related to diagnosed storage in the SRB from early spring to the fall. Deviations from this relationship in winter apparently reflect storage as snow, and are quantitatively consistent with climatological snow water equivalent data for the basin. A simple lumped water balance model of the SRB based on these diagnostic calculations can capture 99% of the mean annual cycle and about 75% of the full variation in monthly-mean flow at the mouth of the Susquehanna River from 1900 to 1987. Unfortunately, only about half of the *interannual* variability at monthly timescales is captured by the model. Thus, monthly predictions of streamflow for a doubling of $CO_2$ have errors as large as the predictions themselves. Despite the large errors, the water balance model illustrates the potential for high sensitivity of streamflow to climate: summertime increases greater than 50% are predicted for a number of climate change scenarios. Improving the skill in predicting the full historical monthly streamflow record is needed so that greater confidence can be placed in climate change predictions for the Susquehanna River and the Chesapeake Bay. This will most likely be achieved by employing models that resolve the large spatial variations of the climate and hydrology of the SRB.

## Acknowledgements

Greg Jenkins kindly made available his nested climate model simulations of the SRB. The support of Ann Fisher and Jim Shortle is greatly appreciated. Thanks to Ana Barros, Tom Cronin, Toby Carlson, Chris Duffy, Dave DeWalle, Barry Evans, Jim Lynch, Doug Miller, Egide Nizeyimana, Dork Sahagian and Zhongbo Yu for helpful discussions and input. This research was supported by the US Environmental Protection Agency through Grant #R824995 to Johns Hopkins University, subcontracted to the Pennsylvania State University under Purchase Order #63629.

## References

Baker, C.B., Eischeid, J.K., Karl, T.R., Diaz, H.F., 1994. The quality control of long-term climatological data using objective data analysis. Preprints of AMS Ninth Conference on Applied Climatology, Dallas, Texas, January 15–20 1995.

Church, M.R., Bishop, G.D., Cassell, D.L., 1995. Maps of regional evapotranspiration and runoff/precipitation ratios in the Northeast United States. J. Hydrol. 168, 283–298.

Crane, R.G., Hewitson, B.C., 1998. Doubled $CO_2$ precipitation changes for the Susquehanna Basin: downscaling from the Genesis General Circulation Model. Int. J. Climatology 18, 65–76.

Gleick, P.H., 1986. Methods for evaluating the regional hydrologic impacts of global climatic changes. J. Hydrol. 88, 97–116.

Gleick, P.H., 1987. The development and testing of a water balance model for climate impact assessment: modeling the Sacramento Basin. Water Resour. Res. 23, 1049–1061.

Jackson, D.R., Jesien, R., 1996. Chesapeake bay low flow strategy study. Susquehanna River Basin Commission Publication 175. Harrisburg, PA.

Jenkins, G.S., Barron, E.J., 1997. Global climate model and coupled regional climate model simulations over the eastern United States: GENESIS and RegCM2 simulations. Global and Planetary Change 15, 3–32.

Jensen, M.E., Burman, R.D., Allen, R.G., 1990. Evapotranspiration and Irrigation Water Requirements. American Society of Civil Engineers, New York, NY.

Justić, D., Rabalais, N.N., Turner, R.E., 1996. Effects of climate change on hypoxia in coastal waters: a doubled $CO_2$ scenario for the northern Gulf of Mexico. Limnol. Oceanogr. 41, 992–1003.

Karl, T.R., Riebsame, W.E., 1989. The impact of decadal fluctuations in mean precipitation and temperature on runoff: a sensitivity study over the United States. Climatic Change 15, 423–447.

McCabe, G.J., 1989. A parabolic function to modify Thornthwaite estimates of potential evapotranspiration for the Eastern United States. Phys. Geography 10, 176–189.

McKenney, M.S., Rosenberg, N.J., 1993. Sensitivity of some potential evapotranspiration estimation methods to climate change. Agric. and Forest Meteorol. 64, 81–110.

Meehl, G.A., Washington, W.M., Erickson III, D.J., Briegleb, B.P., Jaumann, P.J., 1996. Climate change from increased $CO_2$ and direct and indirect effects of sulfate aerosols. Geophys. Res. Lett. 23, 3755–3758.

Mitchell, J.F.B., Johns, T.C., Gregory, J.M., Tett, S.F.B., 1995. Climate response to increasing levels of greenhouse gases and sulphate aerosols. Nature 376, 501–504.

Schubel, J.R., Pritchard, D.W., 1986. Responses of the upper Chesapeake Bay to variations in discharge of the Susquehanna River. Estuaries 9, 236–249.

Seliger, H.H., Boggs, J.A., 1988. Long term pattern of anoxia in the Chesapeake Bay Publication 129. Ref. CBP/TRS 24/88. In: Lynch, M.P., Kronme, E.C. (Eds.). Understanding the Estuary: Advances in Chesapeake Bay Research, Chesapeake Research Consortium, Gloucester Point, VA, pp. 570.

Steffen, M., 1990. A simple method for monotonic interpolation in one dimension. Astron. Astrophys. 239, 443–450.

Thornthwaite, C.W., 1948. An approach toward a rational classification of climate. Geograph. Rev. 38, 55–94.

Wilks, D.S., McKay, M., 1994. Atlas of Extreme Snow Water-equivalent for the Northeastern United States Publication No. RR 94-3. Cornell University Press, Ithaca, NY.